# Synthesis and Characterization of Conjugated, n-Dopable, Bithiazole-Containing Polymers

Jeffrey K. Politis and M. David Curtis*

*Department of Chemistry and the Macromolecular Science and Engineering Center, University of Michigan, Ann Arbor, Michigan 48109-1055*

Lebzy Gonzalez and David C. Martin

*Department of Materials Science and Engineering and the Macromolecular Science and Engineering Center, University of Michigan, Ann Arbor, Michigan 48109-1055*

Yi He and Jerzy Kanicki

*Department of Electrical Engineering and Computer Science, University of Michigan, Ann Arbor, Michigan 48109-2108*

*Received February 5, 1998. Revised Manuscript Received April 23, 1998*

Three polymers, poly(4,4′-dinonyl-5,5′-bithiazole-2,2′-diyl-*co*-5-*tert*-butylphenylene-1,3-diyl) (PBBNBT), poly(4,4′-bis(*p*-dodecylphenyl)-2,2′-bithiazole-5,5′-diyl) (PDPBT), and poly(4,4′-dinonyl-2,2′-bithiazole-5,5′-diyl-*co*-ethynylene) (PENBT), have been synthesized. These polymers illustrate the ability to tune polymer properties around a specific chromophore, in this case the bithiazole ring system. Alterations of optical properties and solid-state morphology have been made while the electrochemical behavior characteristic of the bithiazoles, i.e., reversible reduction near −2.0 V and n-dopability resulting in conductivities around $10^2$ S/cm, has been maintained. All three polymers have also been used as the emitting layer in polymer-based LEDs.

## Introduction

Conducting polymers are being tested as alternate materials for more traditional semiconductors in many electronic devices, such as light-emitting diodes (LEDs)[1−5] and field effect transistors (FETs).[6−8] Polymers offer potential advantages over traditional semiconductors due to their ease of preparation, tunabiltiy, and processablity. The most studied of these devices has been the LED. There have been many improvements in LED fabrication since the first crude device, characterized by low efficiency, was reported by the Cambridge group.[5] However, most of the progress focuses on the device itself.[9−14] Because electroluminescence efficiency can only be 25% of the photoluminescence efficiency,[13] it is important to also improve the emitting material.

Recently, a new class of conjugated polymer, poly(alkybithiazole)s, has been reported.[15−17] These polymers exhibit interesting thermochromic effects[16] and electrochemical behavoir.[17] They have shown to be n-dopable, implying that they are n-type conductors. The most studied polymers in LEDs, poly(alkylthiophene)s[18,19] and poly(*p*-phenylene vinylene)s (PPV)s,[1,3,20] are reported to be hole carriers.[21] There is at least one other example of an LED that has been fabricated from an n-dopable polymer.[21]

Poly(alkylbithiazole)s show high degrees of crystallinity in the solid state, including $\pi$-stacking, usually associated with decreased electroluminescence effi-

(1) Burn, P. L.; A. B. H.; Kraft, A.; Bradley, D. D. C.; Brown, A. R.; Friend, R. H. *J. Chem. Soc., Chem. Commun.* **1992**, 32−34.
(2) Gabriele Grem, G.; Ullrich, B.; Leising, G. *Adv. Mater.* **1992**, *4*, 36−37.
(3) Heeger, D. B. a. A. J. *Appl. Phys. Lett.* **1991**, *58*, 1982−1984.
(4) Cimrova, M. R., V.; Neher, D.; Wegner, G. *Adv. Mater.* **1996**, *8*, 146−149.
(5) Burroughs, D. D. C. B., J. H.; Brown, A. R.; Marks, R. N.; Friend, R. H.; Burn, P. L.; Holmes, A. B. *Nature* **1990**, *347*, 539.
(6) Horowitz, G. *Adv. Mater.* **1996**, *8*, 177−179.
(7) Dodabalapur, H. E. K., A.; Torsi, L.; Haddon, R. C. *Science* **1995**, *269*, 1560−1562.
(8) Rothberg, A. J. L. a. L. J. *J. Mater. Res.* **1996**, *11*, 1581−1591.
(9) Adachi, C.; Tsutsui, T.; Saito, S. *Appl. Phys. Lett.* **1990**, *56*, 799.
(10) Pei, Q.; Yang, Y. *Chem. Mater.* **1995**, *7*, 1568.
(11) Strukelj, M.; Papadimitrakopoulos, F.; Miller, T. M.; Rothberg, L. J. *Science* **1995**, *267*, 1969.
(12) Burrows, P. E.; Forrest, S. R. *Appl. Phys. Lett.* **1994**, *64*, 2285.
(13) Holmes, A. B.; Bradley, D. D. C.; Brown, A. R.; Burn, P. L.; Burroughs, J. H.; Friend, R. H.; Greenham, N. C.; Gymer, R. W.; Halliday, D. A.; Jackson, R. W.; Kraft, A.; Martens, J. H. F.; Pichler, K.; Samuel, I. D. W. *Synth. Met.* **1993**,*55−57*, 4031.
(14) Campbell, I. H.; Joswick, M. D.; Parker, I. D. *Appl. Phys. Lett.* **1995**, *67*, 3137.
(15) Yamamoto, T.; Suganuma, H.; Maruyama, T.; Kubota, K. *J. Chem. Soc. Chem. Commun.* **1995**, 1613.
(16) Nanos, J. I.; Kampf, J. W.; Curtis, M. D.; Gonzalez, L.; Martin, D. C. *Chem. Mater.* **1995**, *7*, 2232.
(17) (a) Yamamoto, T.; Suganuma, H.; Maruyama, T.; Inoue, T.; Muramatsu, Y.; Arai, M.; Komarudin, D.; Ooba, N.; Tomaru, S.; Sasaki, S.; Kubota, K. *Chem Mater.* **1997**, *9*, 1217. (b) Curtis, M. D.; Cheng, H.; Nanos, J. I.; Nazri, G. A., *Macromolecules* **1998**, *31*, 205. (c) Curtis, M. D.; Cheng, H. Johnson, J. A.; Nanos, J. I.; Kasim, R.; Elsenbaumer, R. L.; Gonzalez, L.; Martin, D. C. *Chem. Mater.* **1998**, *10*, 13.
(18) Berggren, M.; Inganäs, O.; Andersson, M. R.; Wennerstrom, O.; Hjertberg, T. *Appl. Phys. Lett.* **1994**, *65*, 1489−1491.
(19) Yamamoto, T.; Miyazaki, Y.; *Chem. Lett.* **1994**, 41−44.
(20) Pei, Q.; Zhang, C.; Yang, Y.; Heeger, A. J. *Science* **1995**, *269*, 1086−1088.
(21) Yamamoto, T.; Sugiyama, K.; Kushida, T.; Inoue, T.; Kanbara, T. *J. Am. Chem. Soc.* **1996**, *118*, 3930.

S0897-4756(98)00074-X CCC: $15.00 
Published on Web 06/15/1998

ciency.[22−24] Poly(nonylbithiazole) (PNBT), which shows three distinct morphologies, each with a different degree of order, is a good illustration of this phenomenon: the more crystalline the phase, the weaker the photoluminescence.[16] Alterations of the polymer backbone can be used to decrease crystallinity and $\pi$-stacking, but with the incorporation of the bithiazole moiety, these new materials should still be n-type transporters. Also, the violet fluorescence of the bithiazole ring system allows access into the entire spectrum of colors by changing the conjugation length.

Herein, the synthesis and characterization of three polymers based on the bithiazole ring system are reported. The polymer backbones have been altered in different fashions to show the tunability of solid-state morphology and emission color of polymers with the bithiazole ring system.

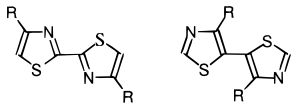


2,2'-bithiazole 5,5'-bithiazole

## Experimental Section

**Materials.** All manipulations and polymerizations were performed under a nitrogen atmosphere using standard Schlenk line techniques unless otherwise stated. Reagent grade solvents were dried and distilled prior to use as described: toluene, tetrahydrofuran (THF), and diethyl ether ($Et_2O$) from Na/benzophenone; dichloromethane ($CH_2Cl_2$) from $CaH_2$; acetonitrile ($CH_3CN$) was dried twice over 3 Å molecular sieves and distilled from boronic anhydride. $Ni(COD)_2$ (COD = cyclooctadiene) was synthesized according to the literature procedure.[25] Reagents were purchased and used as received unless otherwise stated.

$^1$H NMR spectra were collected on a Bruker AM-360, AM-300, or AM-200 and referenced to the residual proton solvent resonance. UV/vis spectra were collected on a Shimadzu 3101PC with baseline correction. Emission spectra were collected on a Shimadzu 4121 interfaced with a Gateway computer. FT-IR spectra were collected on a Bio-Rad FTS-40. X-ray diffraction data were obtained on a Rigaku Rotaflex diffractometer operated at 40 kV, 100 mA, equipped with a Cu target (0.154 nm) and a graphite monochromator. Samples were scanned from 3 to 35° ($2\theta$) at 0.01° intervals and a rate of 1°/min. Cyclic voltammetry (CV) was run using a home-built potentiostat, designed by Wayne Burkhardt, Electronics Shop, Department of Chemistry, University of Michigan, interfaced to a PC computer with a program custom written by Dr. S. Paras, Department of Chemistry, University of Michigan. The solvent was dry acetonitrile and the supporting electrolyte was tetrabutylammonium hexafluorophosphate (0.1 M). Films were cast on a platinum working electrode. The reported potentials are vs the ferrocene/ferrocenium ($Fc/Fc^+$) couple, obtained by adding a crystal of ferrocene to the solution. Two-probe conductivity measurements were performed with a Keithley 617 electrometer on polymer films metallized by evaporation of aluminum. Elemental analysis were performed by either Galbraith Laboratories or the University of Michigan Microanalysis Laboratory.

**Synthesis of 4,4′-Dinonyl-2,2′-bithiazole (NBT).** The procedure described by Nanos was employed.[16] Yield = 6.17 g (72.9%). $^1$H NMR ($CDCl_3$): $\delta$ 0.88 (6 H, t, $J$ = 6.5 Hz), 1.24−1.31 (24 H, m) 1.73 (4 H, m, $J$ = 7.1 Hz), 2.81 (4 H, t, $J$ = 7.7 Hz), 6.92 (2 H, s).

**Synthesis of 5,5′-Diiodo-4,4′-dinonyl-2,2′-bithiazole ($I_2$-NBT).** A dry 250 mL Schlenk flask equipped with a stir bar and $N_2$ inlet/outlet was charged with dry THF (50 mL). The flask was cooled to −78 °C and BuLi (2.45 M in hexanes, 4.26 mL, 10.46 mmol) was added. NBT (2.00 g, 4.75 mmol) in THF (75 mL) was added dropwise via cannula. The dark solution was stirred at room temperature for 2.5 h, and $I_2$ (2.77 g, 10.93 mmol) in THF (75 mL) was added dropwise over 20 min. The reaction was stirred for an additional 1 h and washed with $Na_2S_2O_5$ (saturated, 2 × 100 mL). The light brown solution was dried over $MgSO_4$ and decolorized with carbon. The solvent was removed under reduced pressure to give an oil which solidifies upon standing. The solid was recrystallized twice from $CH_3CN/CHCl_3$ (2:1) to give yellow crystals. Yield = 1.60 g (50.2%). $^1$H NMR ($CDCl_3$): $\delta$ 0.88 (6 H, t, $J$ = 6.4 Hz), 1.26−1.34 (24 H, m), 1.70 (4 H, m, $J$ = 6.6 Hz), 2.77 (4 H, t, $J$ = 7.6 Hz). $\lambda_{max}$(ex) = 244 nm, 362 nm. $\lambda_{max}$(em) = 444 nm. Anal. Calcd for $C_{24}H_{38}I_2N_2S_2$: C, 42.86; H, 5.71; N, 4.17. Found: C, 43.12; H, 5.51; 4.17.

**Synthesis of 1,3-Bis(2-(4-nonylthiazole))-5-*tert*-butylbenzene (BBNBT).** A dry 100 mL Schlenk flask equipped with a stir bar and condenser was charged with the 1,3-bis-(thioamide)-5-*tert*-butylbenzene[26] (0.816 g, 3.23 mmol) and 1-bromoundecanone (1.65 g, 6.63 mmol) in dry DMF (30 mL). The yellow solution was refluxed for 23.5 h. The reaction mixture was allowed to cool and placed into a freezer. The tan crystals were collected and dried under vacuum. Yield = 1.505 g (84.3%). $^1$H NMR ($CDCl_3$): $\delta$ 0.88 (6 H, t, $J$ = 6.7 Hz), 1.28−1.39 (24 H, m), 1.43 (9 H, s), 1.78 (4 H, m, $J$ = 7.1 Hz), 2.85 (4 H, t, $J$ = 7.7 Hz), 6.89 (2 H, s), 8.02 (2 H, d, $J$ = 1.5 Hz), 8.24 (1 H, t, $J$ = 1.5 Hz).

**Synthesis of 1,3-Bis(2-(5-bromo-4-nonylthiazole))-5-*tert*-butylbenzene ($Br_2$-BBNBT).** A 250 mL three-neck flask equipped with a condenser, addition funnel, stir bar, and $N_2$ inlet/outlet was charged with BBNBT (5.51 g, 0.01 mol) in $CHCl_3$ (50 mL). Bromine (3.42 g, 0.0214 mol) in $CHCl_3$ (50 mL) was added dropwise, and the dark solution was refluxed for 22 h. The dark solution was cooled and washed with $Na_2CO_3$ (saturated, 100 mL) and $NaHSO_3$ (saturated, 100 mL). The solution was heated over decolorizing carbon and dried over $MgSO_4$. The solvent was removed in a rotary evaporator to yield a brown oil. The material was recrystallized twice from ethanol to give a white solid. Yield = 2.94 g (41.4%). $^1$H NMR ($CDCl_3$): $\delta$ 0.88 (6 H, t, $J$ = 5.9 Hz), 1.27−1.41 (24 H, m), 1.42 (10 H, s), 1.76 (4 H, m, $J$ = 7.3 Hz), 2.79 (4 H, t, $J$ = 7.6 Hz), 7.91 (2 H, d, $J$ = 1.6 Hz), 8.07 (1 H, t, $J$ = 1.5 Hz). $\lambda_{max}$(ex) = 307 nm, 232 nm. $\lambda_{max}$(em) = 373 nm. Anal. Calcd for $C_{34}H_{50}Br_2N_2S_2$: C, 57.45; H, 7.10; N, 3.94. Found: C, 57.49; H, 7.17; N, 3.74.

**Synthesis of 4,4′-Bis(*p*-dodecylphenyl)-2,2′-bithiazole (DPBT)**. A 100 mL Schlenk flask equipped with a stir bar, condenser, and $N_2$ inlet/outlet was charged with 1-(bromoacetyl)-4-dodecylbenzene (6.89 g, 18.9 mmol) and dithiooxamide (1.07 g, 8.9 mmol) in DMF (80 mL). The reaction mixture was heated to reflux for 1 h and at 60 °C for 5 h. The reaction was allowed to cool and placed into a freezer. The brown crystals were collected and recrystallized from $CH_3CN/CHCl_3$ (3:1) to give tan crystals. Yield = 4.48 g (76.6%). $^1$H NMR ($CDCl_3$): $\delta$ 0.88 (6 H, t, $J$ = 5.6 Hz), 1.26−1.32 (36 H, m), 1.65 (4 H, m, $J$ = 7.4 Hz), 2.65 (4 H, t, $J$ = 7.6 Hz), 7.27 (4 H, d, $J$ = 6.9 Hz), 7.53 (2 H, s), 7.89 (4 H, d, $J$ = 7.8 Hz).

**Synthesis of 5,5′-Dibromo-4,4′-bis(*p*-dodecylphenyl)-2,2′-bithiazole ($Br_2$-DPBT).** The procedure for $Br_2$−BBNBT was followed with some modifications. The reaction was carried out at room temperature, and the solid product was recrystallized twice from $CH_3CN/CHCl_3$ (2:1). Yield = 3.39 g (79.2%). $^1$H NMR ($CDCl_3$): $\delta$ 0.88 (6 H, t, 6.7 Hz), 1.26−1.32 (36 H, m), 1.66 (4 H, m, $J$ = 7.1 Hz), 2.67 (4 H, t, $J$ = 7.6 Hz),

(22) Uchida, M.; Ohmori, Y.; Morishima, C.; Yoshino, K. *Synth. Met.* **1993**,*55−57*, 4168 1993.
(23) Doi, S.; Kuwabara, M.; Noguchi, T.; Ohnishi, T. *Synth. Met.* **1993**, *55−57*, 4174.
(24) Xu, B.; Holdcroft, S. *SPIE*, **1993**, *1910*, 65. Xu, B.; Holdcroft, S. *Macromolecules* **1993**, *26*, 4457.
(25) Schunn, R. A. *Inorg. Synth., Olefin Complexes* **1978**, 5.
(26) Fairfull, A.; Lowe, J. L.; Peak, D. A. *J. Chem. Soc.* **1952**, 742−744.

7.29 (4 H, d, $J$ = 8.2 Hz), 7.90 (4 H, d, $J$ = 8.2 Hz). $\lambda_{max}$(ex) = 262 nm, 367 nm. $\lambda_{max}$(em) = 432 nm. Anal. Calcd for $C_{42}H_{58}Br_2N_2S_2$: C, 61.90; H, 7.19; N, 3.44. Found: C, 62.10; H, 7.21; N, 3.41.

**Synthesis of Poly(4,4′-dinonyl-2,2′-bithiazole-5,5′-diyl-*co*-ethynylene) (PENBT).** A dry 100 mL Schlenk flask equipped with a stir bar and $N_2$ inlet/outlet was charged with $Pd(dba)_2$ (0.04 g, 0.07 mmol) and triphenylphosphine (0.092 g, 0.35 mmol). Dry toluene (60 mL) was added and the system was froze−pumped−thawed. The mixture was allowed to warm to room temperature and stirred until the yellow catalyst color was formed. The solution was transferred via cannula to a dry 100 mL Schlenk flask equipped with a stir bar and $N_2$ inlet/outlet containing $I_2$−NBT (1.5721 g, 2.34 mmol) and 1,2-bis(trimethyltin)acetylene (0.8220, 2.34 mmol), and a condenser was placed on the flask. The reaction mixture was heated to reflux for 26 h, during which time the fluorescence changed from violet to yellow. The red mixture was precipitated by addition to 5% HCl in MeOH (450 mL). The red solid was collected and reprecipitated from toluene into 5% HCl in MeOH (600 mL). The red powder was collected and dried under vacuum at 50 °C. Yield = 0.62 g (59.6%). $^1$H NMR ($CDCl_3$): $\delta$ 0.80−0.90 (6 H, br), 1.20−1.48 (24 H, m) 1.75−1.86 (4 H,br), 2.88−2.95 (4 H, br). $\lambda_{max}$(ex) = 503 nm (film), 475 nm (soln). $\lambda_{max}$(em) = 600 nm (film), 532 nm (soln). Anal. Calcd for $C_{26}H_{38}N_2S_2$: C, 70.52; H, 8.87; N, 6.33. Found: C, 65.62; H, 8.01; N, 5.44; I, 5.09. (Note: implies H(ENBT)$_5$I.)

**Synthesis of Poly(4,4′-bis(*p*-dodecylphenyl)-2,2′-bithiazole-5,5′-diyl) (PDPBT)**. A dry 100 mL Schlenk flask equipped with a stir bar and $N_2$ inlet/outlet was charged with 5,5′-dibromo-4,4′-bis(*p*-dodecylphenyl)-2,2′-bithiazole (1.597 g, 1.96 mmol), $Ni(COD)_2$ (0.72 g, 2.55 mmol), and 2,2′-bypyridyl (0.41 g, 2.65 mmol) in dry toluene (20 mL). A condenser was placed on the flask and the reaction was heated to reflux overnight. The dark, viscous mixture was precipitated by addition of 5% HCl in MeOH (400 mL). The light green solid was collected and redissovled in hot toluene (100 mL). The mixture was filtered through a $^1/_4$ in. plug of Celite, and the solvent volume was reduced to 50 mL. The solution was added to 5% HCl in MeOH (400 mL). The yellow precipitate was collected and stirred in warm 7% EDTA disodium salt in $H_2O$ (300 mL) to remove any remaining Ni salts. The solid was filtered and washed with warm $H_2O$. The polymer was redissolved in hot toluene (100 mL), and the solution was filtered through a $^1/_4$ in. plug of Celite. The solvent volume was reduced to 50 mL, and the polymer was precipitated into MeOH (400 mL). The fluffy yellow solid was dried under vacuum at 50 °C. Yield = 0.806 g (62.8%). $^1$H NMR ($CDCl_3$): $\delta$ 0.80−0.88 (6 H, br), 1.10−1.45 (36 H, m), 1.55−1.67 (4 H, br), 2.53−2.65 (4 H, br), 7.02−7.15 (4 H, br), 7.67−7.75 (4 H, br). $\lambda_{max}$(ex) = 420 nm (film), 417 nm (soln). $\lambda_{max}$(em) = 511 nm (film), 504 nm (soln). Anal. Calcd for $C_{42}H_{50}N_2S_2$: C, 77.00; H, 8.94; N, 4.28. Found: C, 77.04; H, 9.02; N, 4.19.

**Synthesis of Poly(4,4′-dinonyl-5,5′-bithiazole-2,2′-diyl-*co*-5-*tert*-butylphenylene-1,3-diyl) (PBBNBT).** A 100 mL Schlenk flask equipped with a stir bar and $N_2$ inlet/outlet was charged with $Br_2$−BBNBT (1.01 g, 1.42 mmol), $Ni(COD)_2$ (0.523 g, 1.85 mmol), and 2,2′-bypyridyl (0.300 g, 1.92 mmol) in dry toluene (14 mL). A condenser was placed on the flask and the reaction mixture was heated to reflux. After 20 h, the dark solution was precipitated by addition to 5% HCl in MeOH (400 mL). The light green solid was collected and redissolved in toluene (60 mL). The mixture was filtered through a $^1/_4$ in. plug of Celite and added to 5% HCl in MeOH (400 mL). The light yellow precipitate was collected and stirred in a warm solution of 7% EDTA disodium salt in $H_2O$ (300 mL). The solid was collected and dissolved in $CHCl_3$ (75 mL), and the mixture was filtered through a $^1/_4$ in. plug of Celite. The solvent volulme was reduced to 50 mL, and the polymer was precipitated by addition to MeOH (400 mL). The slightly stringy solid was collected and dried under vacuum to give a pale yellow material. Yield = 0.423 g (54.0%). $^1$H NMR ($CDCl_3$): $\delta$ 0.82 (6 H, t, $J$ = 5.8 Hz), 1.20−1.40 (24 H, m), 1.46 (10 H, s), 1.76−1.86 (4 H, m), 2.76 (4 H, t, $J$ = 7.0 Hz), 8.05 (2 H, d, $J$ = 1.5 Hz), 8.30 (1 H, t, 1.5 Hz). $\lambda_{max}$(ex) = 338 nm (film), 337 nm (soln). $\lambda_{max}$(em) = 452 nm (film), 457 nm (soln). Anal. Calcd for $C_{34}H_{50}N_2S_2$: C, 74.11; H, 9.17; N, 5.09. Found: C, 74.69; H, 9.30; N, 5.05.

**Scheme 1. Synthesis of PDPBT**

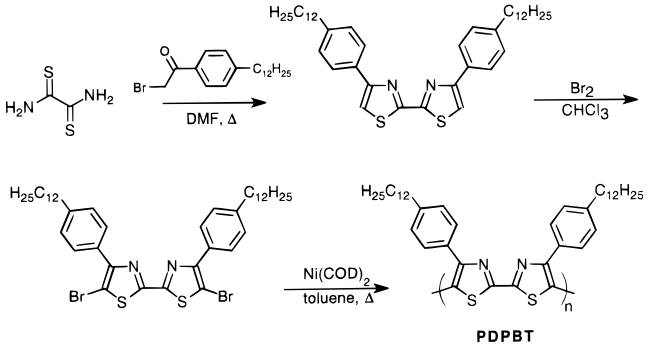


**Scheme 2. Synthesis of PBBNBT**

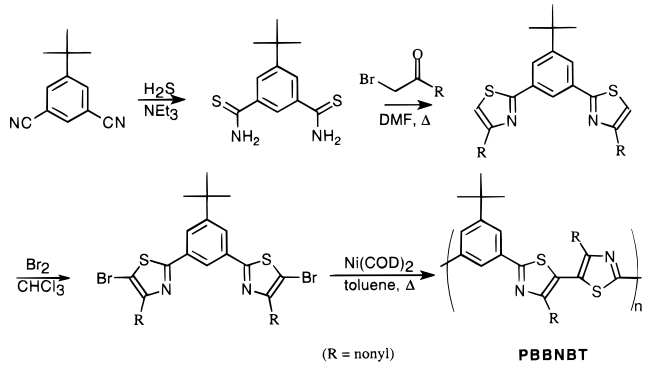


**Scheme 3. Synthesis of PENBT**

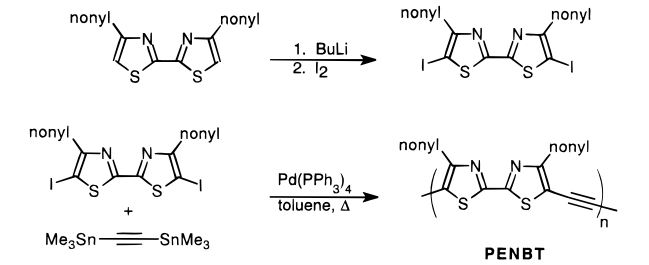


## Results and Discussion

**Preparation**. Poly(bithiazole)s, both homopolymers and copolymers, were readily synthesized via either nickel- or palladium-mediated coupling reactions. The first route utilized a zero-valent nickel complex to couple aryl bromides.[27] Both poly(4,4′-bis(*p*-dodecylphenyl)-2,2′-bithiazole-5,5′-diyl) (PDPBT) (Scheme 1) and poly(4,4′-dinonyl-5,5′-bithiazole-2,2′-diyl-*co*-5-*tert*-butylphenylene-1,3-diyl) (PBBNBT) (Scheme 2) were obtained in this manner in good yields. Poly(4,4′-dinonyl-2,2′-bithiazole-5,5′-diyl-*co*-ethynylene) (PENBT) (Scheme 3) was prepared via a Stille[28] coupling of 5,5′-diiodo-4,4′-dinonyl-2,2′-bithiazole and 1,2-bis(trimethyltin)acetylene. In all cases, dry toluene was used for the polymerizations as the polymers are insoluble in more polar

(27) Yamamoto, T.; Maruyama, T.; Zhou, Z.; Ito, T.; Fukuda, T.; Yoneda, Y.; Begum, F.; Ikeda, T. S.; Tahezoe, H.; Fukuda, A.; Kubota, K. *J. Am. Chem. Soc.* **1994**, *116*, 6, 4832.

(28) Stille, J. K.; Simpson, E. *J. Am. Chem. Soc.* **1987**, *109*, 2138.

**Table 1. Optical, Molecular Weight, and Thermal Characterization**

| polymer | $\lambda_{max}$ (nm) absorb.[a] | $\lambda_{max}$ (nm) emission[b] | optical band[c] gap (eV) | mol wt[d] (kDa) | TGA[e] 5 wt % loss |
|---|---|---|---|---|---|
| PBBNBT | 337 (soln) | 457 (soln) | 2.91 | $M_n = 16.6$ | 545 °C |
| | 338 (film) | 452 (film) | | PDI = 6.7 | |
| PDPBT | 417 (soln) | 504 (soln) | 2.65 | $M_n = 52.0$ | 542 °C |
| | 420 (film) | 511 (film) | | PDI = 3.8 | |
| PENBT | 475 (soln) | 532 (soln) | 2.00 | $M_n = 2.1$ | 310 °C |
| | 503, 553 (sh) (film) | 600 (film) | | PDI = 22.8 | |

[a] Solution spectra were taken with chloroform as the solvent at ambient temperature. [b] Emission excitation at $\lambda_{max}$(abs) in $CHCl_3$ solution. [c] The optical band gap was taken from the films' absorbance spectra by extrapolation to $A = 0$ of the low energy slope. [d] GPC using $CHCl_3$ as the eluent and polystyrene standards. [e] TGAs were performed under nitrogen at a 40 °C/min heating rate.

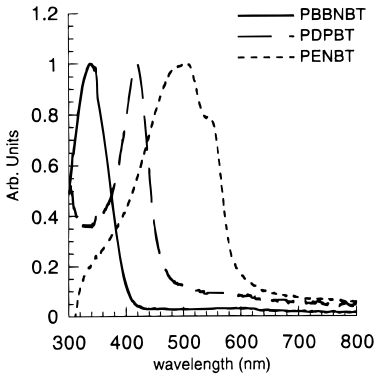


**Figure 1.** Absorbance spectra of the polymer films.

solvents. Table 1 summarizes the characterization of the polymers.

These synthetic routes allow access to a variety of polymers which can be altered in a number of ways, as demonstrated by the three polymers described here. Substituting the side chains on the bithiazole ring with various alkyl and aryl groups is relatively simple, and therefore, a series of homopolymers, e.g., PDPBT, can be synthesized. Polybithiazoles with other substituents have recently been reported.[17] Copolymers with bithiazole can also be prepared. Two different methods were investigated. The first was a more traditional approach wherein two monomers were coupled together using the Stille coupling as in PENBT. In the second pathway, both monomers were incorporated into a single molecule, which was then polymerized like the homopolymers. PBBNBT was designed in this fashion. The chemistry behind the poly(bithiazole)s is straightforward and allows tailoring of the polymers to provide desirable characteristics, e.g. good luminescence, good film forming ability.

**Optical Data**. In all cases, the polymerization of the monomer increased the $\pi$-conjugation length. However, the amount of this extension varied with each polymer. The absorbance band of PBBNBT shifted by only 30 nm, going from 307 nm in the monomer to 337 nm in the polymer. With PDPBT, the absorbance maximum shifted 50 nm, from 367 to 417 nm. PENBT shows the largest red shift, 113 nm, from 362 nm (NBT) to 475 nm in the polymer.

Figure 1 shows the normalized UV/vis spectra of the polymer thin films. The red shift in $\lambda_{max}$ of the absorbance spectra shows that the order of increasing conjugation length is PBBNBT < PDPBT < PENBT. For PBBNBT, the conjugation is interrupted by the meta linkages of the phenyl rings. Hence the polymer's maximum conjugation length is likely to incorporate only two phenyl rings bridged by one bithiazole moiety. In the case of PDPBT, the conjugation length is controlled by the steric bulk of the dodecylphenyl substituent. A recent study of poly(alkylbithiazole)s shows that as larger substituents are placed on the bithiazole rings, the absorption wavelength of the films reaches a plateau around 420 nm, and eventually decreases to a minimum of 382 nm.[17a] This is due to the rings being forced out of planarity from steric hindrance. In the case of PENBT, the acetylene bridge between the NBT units serves to continue the conjugation and provides a spacer between long alkyl chains, thus avoiding the steric problems seen in PDPBT.

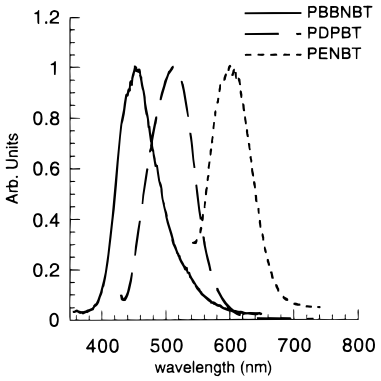


**Figure 2.** Emission spectra of the polymer films.

It is generally recognized that photoluminescence (PL) and electroluminescence (EL) arise from the lowest energy singlet exciton.[13] This means that the color of an LED normally matches the fluorescence spectrum of the material. The violet emission of the bithiazole moiety allows access to the full visible spectrum by decreasing the HOMO−LUMO gap. Higher energy emissions are obtained by isolating the fluorophore into a nonconjugated backbone, whereas the longer wavelengths, down to the red, are obtained by increasing the effective conjugation lengths. The three polymers reported here illustrate the tunability of the color of light emitted from the bithiazole moiety. Figure 2 shows the emission spectra of the polymer films. PBBNBT emits a blue-green light ($\lambda_{max}$ (film) = 452 nm) while a low-energy, deep red color ($\lambda_{max}$ (film) = 600 nm) is emitted from PENBT. PDPBT falls in the middle with a yellow-green fluorescence ($\lambda_{max}$ (film) = 511 nm). Thus LEDs made from these polymers are expected to show a similar spectrum of colors.

**Solid-State Structure.** Solid-state morphology of polymers plays a major role in the performances of polymer-based devices, e.g. LEDs and TFTs. In solution, when the concentration of the chromophore increases, the fluorescence intensity decreases.[29] Similarly, intermolecular $\pi-\pi$ stacking leads to the formation of exciplexes that greatly decrease the quantum efficiency of LEDs.[22−24] Conversely, such stacking is expected to decrease the activation energy for electron

(29) Tinoco, Jr., I.; Sauer, K.; Wang, J. *Physical Chemistry: Principles and Applications in Biological Sciences*; Prentice-Hall: Englewood Cliffs, New Jersey, 1985.

hopping and may lead to higher carrier mobilities and better performance in TFTs.[30−32]

Hence, desirable polymer characteristics depend critically on the intended application, so that understanding and controlling polymer morphology is critical to optimizing device performance. Regioregularity, small steric bulk, and main chain planarity all favor $\pi-\pi$ stacking,[16,33,34] whereas bulky substituents and regioirregularity inhibit $\pi-\pi$ stacking. Hence, for high luminescent efficiency, materials should be amorphous or "solution-like" in the solid state.

One method of examining the "solution-like" behavior of solids is to compare the optical properties of the polymer in solution verses the film. Both PBBNBT and PDPBT show little change in their absorbance spectra in going from solution to film, implying that the polymers adopt the same molecular conformation in both solution and solid film. These results are in contrast to films of PNBT, which show red shifts (vs solution) due to increased planarity and conjugation length, as well as additional red shifts caused by $\pi$-stacking. PENBT, however, has a more complicated absorbance spectrum. First, it does not adopt the same morphology in the film as in solution, as evidenced by the 28 nm shift (Table 1). Interestingly, the solid-state spectra (Figure 1) is further complicated by the appearance of a shoulder at longer wavelength ($\lambda_{max}$ (film) = 553 nm), in addition to the major peak ($\lambda_{max}$ (film) = 503 nm). This phenomenon has been observed before in the solid-state spectra of regioregular poly(3-alkylthiophene),[34] NBT oligomers, and 2,5-disubstituted PPPs.[35] Currently, the nature of this low-energy absorbance is not well-understood, but is under investigation.[36]

The emission data (Table 1) of the polymers also give some insight into the solid-state structure. Again, PENBT shows a substantial red shift from solution to solid state, consistent with an ordered, more planar structure in the solid. In the solid, the exciton can migrate either along a chain or to neighboring chains until it is pinned to a low-energy region (long, planar segment). Neither the PDPBT nor the PBBNBT shows any shift in the emission spectra from the solutions to the films. In the case of PBBNBT, the meta linkage and the *tert*-butyl groups in the polymer backbone force a solid-state morphology that is "solution-like". The dodecylphenyl substituents on PDPBT have seemingly produced the same effect.

From the optical data, it appears that PBBNBT and PDPBT do not form $\pi$-stacks in the solid state. However, the X-ray diffraction (XRD) of the polymer films provides more conclusive evidence. Figure 3 is a plot of the XRD data. PDPBT shows a large degree of crystallinity in lamellar spacing ($d$ = 25 Å), most likely due to side chain crystallization. However, none of the polymers exhibit a peak at $2\theta = \sim 25°$, which is indicative of interchain stacking ($d$ = 3.5 Å). From the XRD data, it is apparent that PBBNBT is nearly completely amorphous. Although not present in the initially cast film, $\pi$-stacking can be induced by pressure in PENBT, which also induces a corresponding color change. Figure 4 compares the XRD of both pressed, green in appearance, and unpressed, red in appearance, PENBT. This piezochromism will be discussed in a future article.[36]

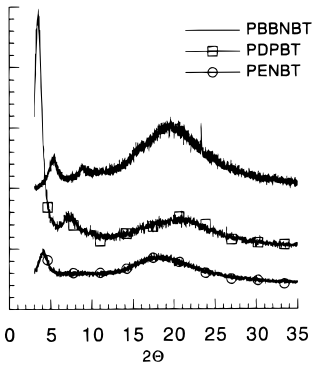


**Figure 3.** XRD curves of the polymer films.

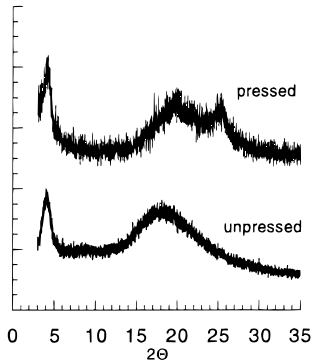


**Figure 4.** XRD curves for unpressed and pressed PENBT.

**Table 2. Cyclic Voltammetry of Polymer Films**[a]

| | $E^{1/2}_{red}$ (V)[b] | $\Delta E^{P}_{red}$ (V) | $E^{P}_{ox}$ (V) | $\Delta E_{ox-red}$ (V) |
|---|---|---|---|---|
| PBBNBT | −2.41 | 0.23 | 1.18 | 3.59 |
| PDPBT | −1.94 | 0.26 | 1.56 | 3.50 |
| PENBT | −1.87 | 0.06 | 1.31 | 3.18 |

[a] Potentials are referenced to $Fc/Fc^+$ (i.e. $E^{1/2}_{Fc/Fc+} = 0.0$ V). [b] $1/2(E^{P}_{R} - E^{P}_{ox})$.

Overall, this information implies that, by changing either the alkyl chain substituent or introducing different spacers between the bithiazole moiety, the solid-state morphology as well as the effective conjugation length are controllable. A rigid spacer between bithiazole moieties decreases the steric constraints of the alkyl chains, allowing for longer conjugation lengths. As longer and/or bulkier substituents or spacers are used, the solid-state conformations become more and more like those present in solution.

**Electrochemical and Electronic Characterization.** Poly(alkylbithiazole)s show a quasi-reversible reduction and an irreversible oxidation.[17a,b] Each of the polymers discussed here exhibit similar electrochemistry with each material having a quasi-reversible reduction and an irreversible oxidation. Table 2 summarizes the cyclic voltammetry results. Figure 5 shows a typical

(30) Miller, L. L.; Zhong, C. J.; Kasai, P. *J. Am. Chem. Soc.* **1993**, *115*, 5982.
(31) Laquindanum, J. G.; Datz, H. E.; Lovinger, A. J.; Dodabalapur, A. *Chem. Mater.* **1996**, *8*, 2542.
(32) Bao, Z.; Feng, Y.; Dodabalapur, A.; Raju, V. R.; Lovinger, A. J. *Chem. Mater.* **1997**, *9*, 1299.
(33) Chen, T.; Wu, X.; Rieke, R. *J. Am. Chem. Soc.* **1995**, *117*, 233.
(34) McCullough, R. D.; Lowe, R. D.; Jayaraman, M.; Anderson, D. L. *J. Org. Chem.* **1993**, *58*, 904.
(35) Vahlenkamp, T.; Wegner, G. *Macromol. Chem. Phys.* **1994**, *195*, 1933.
(36) Blanda, W.; Curtis, M. D.; Francis, A. H., work in progress.

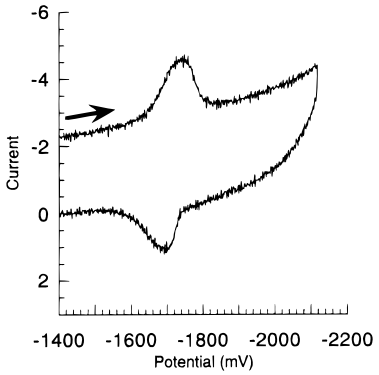


**Figure 5.** Cyclic voltammogram of a PENBT film at a 200 mV sweep rate.

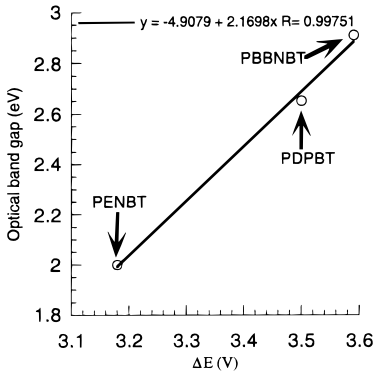


**Figure 6.** Plot of the optical band gap vs the difference in the oxidation and reduction potentials.

voltammogram of the cathodic wave of a solid film cast on the electrode. Repeated sweeps of reduction and reoxidation did not result in changes in the current response, suggesting that the polymers are stable to n-doping. However, once the potential is swept past the oxidation peak near 1.6 V, the film lost electrochemical response, i.e., the polymer film was destroyed. Because each material has a different backbone makeup, the fact that each shows essentially the same electrochemical behavior implies that the electroactive species is most likely the bithiazole ring system. Recent results show that each bithiazole ring in PNBT accepts one electron upon electrochemical reduction at −2.0 V.[17b]

The oxidation potential can be related to the energy level of the HOMO, and the reduction potential stems from the position of the LUMO. In a series of similar compounds, the difference between the oxidation potential and the reduction potential, $\Delta E$, correlates with the optical band gap of the polymers. Such a correlation is expected only when changes in solvation or polarization energies for the different polymers are essentially constant in the series, and the optical transitions are between states for which configuration interaction is not important, etc. As has been observed (or assumed) in many studies,[37−39] a linear relationship exists between $\Delta E$ and the optical band gap of the polymers studied here. Figure 6 shows this relationship, and Figure 7 shows the relative positions of the HOMO and LUMO

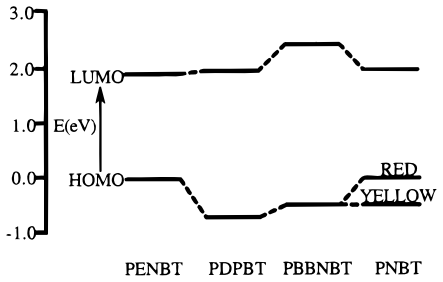


**Figure 7.** Relative energies of the HOMOs and LUMOs as derived from the reduction potential and the optical band gap. PNBT has different band gaps corresponding to different morphologies.[16,17b]

**Table 3. Conductivity (S/cm) of Polymers[a]**

| polymer | neutral[a] | n-doped[b] |
|---|---|---|
| PBBNBT | $4 \times 10^{-14}$ | 4 |
| PDPBT | $5 \times 10^{-14}$ | 135 |
| PENBT | $5 \times 10^{-10}$ | 200 |

[a] Two-point probe at ambient temperature. [b] Calculated from $\sigma = K^2/2\omega\mu_o$.

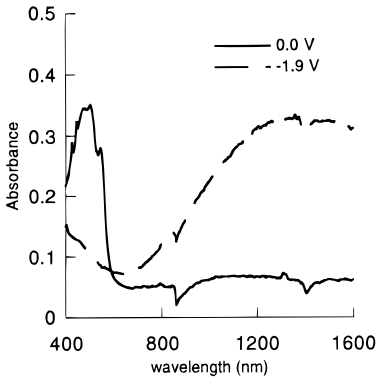


**Figure 8.** UV/vis/NIR spectra of neutral and n-doped PENBT.

for the series of polymers as deduced from the CV and UV/vis data.

Two-probe conductivity measurements on each polymer film have been carried out. Not surprisingly, the neutral polymers are insulators. The graphs of current vs voltage show an ohmic relationship. It is interesting to note that the material with the longest wavelength, PENBT, shows the highest conductivity, while the conductivities of PDPBT and PBBNBT are ca. $10^4$ lower. The "solution-like" solid-state morphology that the latter two polymers show is expected to give low mobilities to the charge carriers, whereas carrier mobility should be enhanced by $\pi$-contacts in PENBT. Table 3 summarizes the results.

**Spectroelectrochemistry.** As with PNBT,[17b] all three polymers are "n-dopable". In an inert atmosphere, a film of the polymer cast onto an ITO-coated glass slide was placed into a quartz cell containing the electrolyte solution. A potential, between −1.9 and −2.0 V (vs Ag wire), was applied and the UV/vis/NIR spectrum was recorded. Figure 8 compares the spectra of the neutral and reduced forms of PENBT. In all cases, the absorbance in the visible region decreased and was replaced by a broad absorption in the NIR due to "free carriers" as the polymers were reduced. The stability of the doped state was ascertained by opening the circuit once the polymers were doped. No changes in the absorption spectra were noted upon standing for 15 min. Closing

(37) Dodabalapur, A.; Katz, H. E.; Torsi, L. *Adv. Mater.* **1996**, *8*, 853.
(38) Wu, C. C.; Sturm, J. C.; Register, R. A.; Tian, J.; Dana, E. P. *IEEE Trans. Electron Devices* **1997**, *44*, 1269.
(39) Ishii, H.; Seki, K. *IEEE Trans. Electron Devices* **1997**, *44*, 1295.

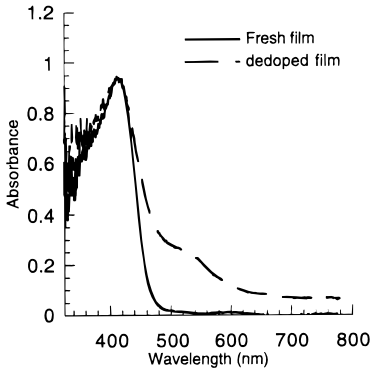


**Figure 9.** UV/vis spectra of neutral PDPBT, both undoped and dedoped.

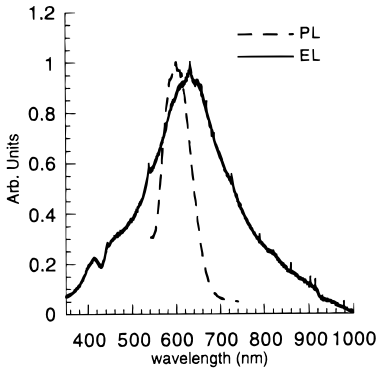


**Figure 10.** Photoluminescence and electroluminescence of PENBT.

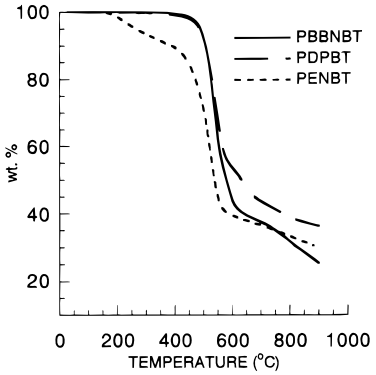


**Figure 11.** TGA of the polymers under nitrogen.

the circuit and applying a 0.0 V potential to discharge the doped film caused the visible peak intensity to increase and the NIR absorption to decrease. Again, as in PNBT, both PBBNBT and PDPBT show an additional peak at longer wavelength after the doping/dedoping process. Figure 9 illustrates this phenomenon for PDPBT. The long wavelength absorption has been ascribed to an induced morphology change caused by swelling and deswelling of the polymers caused by the migration of the dopant ions in to and out of the polymers. Another possible explanation for this phenomenon is the presence of "trapped" doped forms of the polymer imbedded in the neutral insulating polymer.

Due to the reactivity of n-doped polymers, it is difficult to measure their conductivity by traditional two- or four-probe measurements. New, in situ methods for determining the conductivity of doped polymers have been developed. One such method, using a bipotentiostat, measures the conductivity simultaneously with electrochemical doping.[40] This process proved unsuccessful due to the poor adhesion of these polymers to the interdigitated electrode. Another method, based upon the "free electron absorption", uses the molar absorption coefficient of the NIR absorbance to calculate the conductivity.[41] Using the Drude equation, $K = (2\sigma\omega\mu_o)^{1/2}$, where $K$ = the absorption coefficient ($cm^{-1}$), $\sigma$ = the conductivity, $\omega$ = the frequency of the NIR absorption maximum, and $\mu_o$ = the permeability of free space,[42] the conductivity of the n-doped polymers can be estimated from the spectroelectrochemistry. The values calculated for the polymers are given in Table 3.

**Light-Emitting Diodes.** Crude three-layer devices were fabricated using each polymer as the emitting layer, ITO as the anode, and aluminum as the cathode. The device characteristics were measured in air. Light output was observed from each polymer with a turn-on voltage between 30 and 40 V. Interestingly, for both PENBT and PDPBT, the EL spectrum is red-shifted with respect to the PL spectrum. Figure 10 compares the PL and EL spectra of PENBT. As stated previously, the PL and EL typically overlay; however, it is not surprising that it does not here since, for PENBT and PDPBT, the PL wavelength depends strongly on the excitation wavelength used, varying as much as 100 nm.[36] The breadth of the spectrum is explained by the fact that there are several possible conjugation lengths in the solid state from which the exciton may emit. Further LED characteristics will be discussed in a future article.

**Thermal and Oxidative Stability.** Poly(bithiazole)s are quite robust. Figure 11 shows the thermal decomposition curves of the polymers. Both PBBNBT and PDPBT have decomposition temperatures above 500 °C, while that of PENBT is also high at 310 °C. The cause of the lower decomposition temperature of PENBT has not been characterized, though it could be due to a cross-linking reaction with the loss of a small molecule byproduct. The materials are also oxidatively stable in air. Each polymer was studied closely over time by FT-IR. Subtraction of the spectra over a 1 month period exhibited no new peaks nor any changes in the relative intensities of peaks.

## Conclusions

Several synthetic pathways leading to bithiazole-containing polymers were demonstrated. By varying the side chains and/or spacing groups between the bithiazole rings, some characteristics, such as optical band gap and solid-state morphology, can be altered while other desirable traits, e.g. n-dopability and thermal stability, are maintained

**Acknowledgment.** The authors thank the National Science Foundation (DMR-9510274) for support for this research.

CM980074Y

(40) Ofer, D.; Crooks, R. M.; Wrighton, M. S. *J. Am. Chem. Soc.* **1990**, *112*, 7869.
(41) Feldblum, A.; Kaufman, J. H.; Heeger, A. J. *Phys. Rev. B* **1982**, *26*, 815.
(42) Eliott, R. J.; Gibson, A. F. *An Introduction to Solid State Physics and Its Applications*; The Macmillan Press: Basingstoke, UK, 1974; pp 264−268.